

This paper was presented at the National Academy of Sciences colloquium “Geology, Mineralogy, and Human Welfare,” held November 8–9, 1998 at the Arnold and Mabel Beckman Center in Irvine, CA.

## Surface geochemistry of the clay minerals

GARRISON SPOSITO\*<sup>†</sup>, NEAL T. SKIPPER<sup>‡</sup>, REBECCA SUTTON\*, SUNG-HO PARK\*, ALAN K. SOPER<sup>§</sup>,  
AND JEFFERY A. GREATHOUSE<sup>¶</sup>

\*Earth Sciences Division, Mail Stop 90/1116, Ernest Orlando Lawrence Berkeley National Laboratory, University of California, Berkeley, CA 94720; <sup>†</sup>Department of Physics and Astronomy, University College, Gower Street, London WC1E 6BT, United Kingdom; <sup>§</sup>ISIS Facility, Rutherford Appleton Laboratory, Chilton, Didcot, Oxfordshire OX11 0QX, United Kingdom; and <sup>¶</sup>Department of Chemistry, University of the Incarnate Word, 4301 Broadway, San Antonio, TX 78209

**ABSTRACT** Clay minerals are layer type aluminosilicates that figure in terrestrial biogeochemical cycles, in the buffering capacity of the oceans, and in the containment of toxic waste materials. They are also used as lubricants in petroleum extraction and as industrial catalysts for the synthesis of many organic compounds. These applications derive fundamentally from the colloidal size and permanent structural charge of clay mineral particles, which endow them with significant surface reactivity. Unraveling the surface geochemistry of hydrated clay minerals is an abiding, if difficult, topic in earth sciences research. Recent experimental and computational studies that take advantage of new methodologies and basic insights derived from the study of concentrated ionic solutions have begun to clarify the structure of electrical double layers formed on hydrated clay mineral surfaces, particularly those in the interlayer region of swelling 2:1 layer type clay minerals. One emerging trend is that the coordination of interlayer cations with water molecules and clay mineral surface oxygens is governed largely by cation size and charge, similarly to a concentrated ionic solution, but the location of structural charge within a clay layer and the existence of hydrophobic patches on its surface provide important modulations. The larger the interlayer cation, the greater the influence of clay mineral structure and hydrophobicity on the configurations of adsorbed water molecules. This picture extends readily to hydrophobic molecules adsorbed within an interlayer region, with important implications for clay–hydrocarbon interactions and the design of catalysts for organic synthesis.

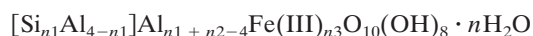
The clay minerals are layer-type aluminosilicates, ubiquitous on our planet in geologic deposits, terrestrial weathering environments, and marine sediments (1, 2). Their name derives from the micrometer-sized particles into which they crystallize. This small particle size, in turn, endows these minerals with an important surface reactivity that plays a major role in the terrestrial biogeochemical cycling of metals, in the chemical homeostasis of the oceans, and in a broad variety of managed processes, including oil and gas production, industrial catalysis, pharmaceutical delivery, and radioactive waste disposal. Metal nutrients such as  $K^+$  or  $Ca^{2+}$  are retained in temperate-zone soils on negatively charged clay mineral surfaces but eventually can be released for consumption in the biosphere or for buffering these soils against excess acidity brought in by applied fertilizers or contaminated rainwater (3). Clay minerals precipitated from seawater in nearshore depositional environments can similarly influence the geochemical cycles of metal cations such as  $K^+$  (4), as well as the oceanic buffering of atmospheric  $CO_2$  on a global scale (5). In engineered settings, clay mineral swelling promoted by  $Na^+$  adsorption plays a significant role in petroleum extraction

(6) and in the construction of environmental liners (7). Major impact on industrial organic synthesis comes in the many designed catalysts developed from clay minerals with adsorbed polymeric cations (8).

Certain clay minerals are isostructural with mica (1, 2) but are not as well crystallized because of random isomorphous cation substitutions in their structure (9, 10). These cation substitutions lead to a negative net surface charge that induces an electrical double layer on clay mineral surfaces when they are exposed to aqueous electrolyte solutions (i.e., to natural waters). Water molecules can be intercalated between clay layers to create an interlayer ionic solution that causes swelling phenomena related to electrical double layer properties (3, 6, 11, 12).

The structure of the double layer that forms in swelling clay mineral interlayers has been the object of much geochemical research (12), but only in recent years, aided especially by insights gained from studies of concentrated aqueous ionic solutions (13), has the powerful tandem mix of spectroscopy and molecular modeling been able to clarify matters. Two particularly effective innovations have been isotopic-difference neutron diffraction and Monte Carlo computer simulation (13). The present article is a brief account of our own recent efforts in applying these two innovations to the hydrated clay minerals, which are of widespread importance in terrestrial surface geochemistry. The emphasis here is on a molecular picture of clay hydrate interlayer structure, particularly the issues of how similar this structure is to that in concentrated ionic solutions and how different it is from the tetrahedral hydrogen-bonded network characteristic of liquid water in bulk. This kind of fundamental understanding is essential to improved modeling of global elemental cycles and better design of engineered clay materials (5–8).

**Crystal Structures of Clay Minerals.** Clay minerals are stacked, polymeric sandwiches of tetrahedral and octahedral sheet structures (3, 9–12). They are classified first into “layer types,” differentiated by the number of tetrahedral and octahedral sheets that have combined, and then into “groups,” differentiated by the kinds of isomorphous cation substitution that have occurred (10). Layer types are sketched in Fig. 1A, and the groups are identified in Table 1. The 1:1 layer type consists of one tetrahedral sheet fused to an octahedral sheet. It is represented in Table 1 by the kaolinite group, whose generic chemical formula is



where cations enclosed in square brackets are located in the tetrahedral sheet, and the stoichiometric coefficients ( $ni$ ,  $i =$

Abbreviation: MC, Monte Carlo.

<sup>†</sup>To whom reprint requests should be addressed at: Hilgard Hall #3110, University of California, Berkeley, CA 94720-3110. e-mail: gposito@nature.berkeley.edu.

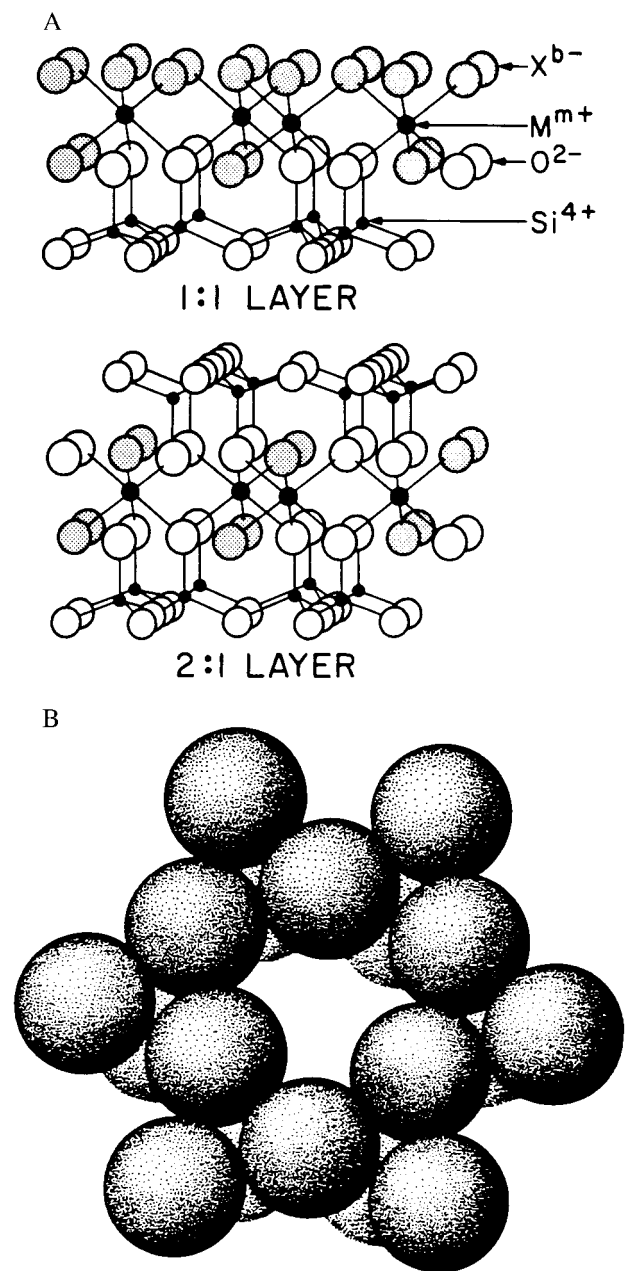
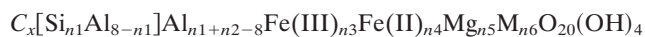


FIG. 1. (A) Crystal structure of 1:1 and 2:1 layer type clay minerals, where X (shaded circles) is usually OH and M can be Al, Mg, Fe, etc. (B) Siloxane cavity in the basal plane of a tetrahedral sheet.

1, 2, 3), which may be fractions, are constrained by charge neutrality and mass balance conditions given in Table 1. The octahedral sheet has two-thirds cation-site occupancy (dioctahedral sheet; full occupancy gives a trioctahedral sheet), and the structural hydration coefficient  $n = 0$ , except for 10-Å halloysite ( $1 \text{ \AA} = 0.1 \text{ nm}$ ), for which  $n = 4$ . Normally, there is no significant isomorphous substitution for Si in the tetrahedral sheet ( $n_1 = 4$ ) or for Al in the octahedral sheet ( $n_2 = 4$ ), and, therefore, no significant negative structural charge occurs in this dioctahedral clay mineral (9, 10).

The 2:1 layer type has two tetrahedral sheets fused to an octahedral sheet. Three clay mineral groups having this structure are illite, vermiculite, and smectite (9, 10). Their generic chemical formula is



where charge and mass balance constraints again appear in Table 1. The symbol  $C_x$  represents  $x$  moles of monovalent cation charge that balances negative structural charge created by isomorphous replacement of tetrahedral Si by Al; dioctahedral Al by Mg, Fe(II); or trioctahedral Mg by the unspecified structural cation M (for example, Li in the trioctahedral mineral hectorite). The layer charge  $x$  is thus the number of moles of excess electron charge per chemical formula unit that is produced by isomorphous cation substitutions (Table 1). It is balanced by cations adsorbed on or near the basal plane of a tetrahedral sheet.

The three 2:1 groups are differentiated in two principal ways. As indicated in Table 1, the layer charge generally decreases in the order illite  $\rightarrow$  vermiculite  $\rightarrow$  smectite. The vermiculite group is further distinguished from the smectite group by a much greater degree of isomorphous substitution in the tetrahedral sheet (9, 10). Among dioctahedral smectites, those for which substitution of Al for Si in the tetrahedral sheet exceeds that of Fe(II) or Mg for Al in the octahedral sheet are called beidellite, and those for which the reverse is true are called montmorillonite (11). The emphasis in the present article will be on vermiculite and smectite clay minerals because of their importance in terrestrial weathering processes and designed industrial applications (5–8).

**Siloxane Surface Reactivity.** The plane of oxygen ions bounding each side of a 2:1 clay mineral layer (i.e., the basal plane of a tetrahedral sheet) is called a siloxane surface (12). A reactive site associated with this surface is the hexagonal cavity formed by the bases of six corner-sharing Si tetrahedra (Fig. 1B). It has a diameter of  $\approx 0.26 \text{ nm}$  and is bordered by six oxygen ions, with a hydroxyl group rooted at the bottom in the octahedral sheet. In dioctahedral clay minerals, this hydroxyl group points toward the empty metal site in the octahedral sheet whereas, in trioctahedral clay minerals, it points perpendicularly to the siloxane surface (9).

The reactivity of the siloxane surface depends on the nature of the local charge distribution in the clay layer (12). In the absence of nearby isomorphous cation substitutions that create negative charge, a siloxane surface functions only as a mild charge donor. If isomorphous substitution of Al by Fe(II) or Mg occurs in the octahedral sheet, the resulting excess negative charge makes it possible for the surface to form reasonably strong adsorption complexes with cations and water molecules. If isomorphous substitution of Si by Al occurs in the tetrahedral sheet, with the excess negative charge thereby localized much nearer to the periphery of the siloxane surface, much stronger adsorption complexes with cations and stronger hydrogen bonds to vicinal water molecules become possible. Charged sites also exist on the edges of clay mineral crystallites (12). Their role in clay mineral surface geochemistry ranges from critical to subordinate as the layer type shifts from 1:1 to 2:1 (9, 11, 12).

Cation adsorption complexes can be classified as either inner-sphere or outer-sphere (3). An inner-sphere surface complex has no water molecule interposed between the surface functional group and the small cation or molecule it binds whereas an outer-sphere surface complex has at least one such interposed water molecule. Outer-sphere surface complexes thus comprise solvated adsorbed cations. Surface complexes involving metal cations are illustrated in Fig. 2 for a 2:1 layer type clay mineral.

Ions bound in surface complexes are distinguished from those adsorbed in the diffuse portion of the electrical double layer (also illustrated in Fig. 2) because the former species remain immobilized on a siloxane surface over molecular time scales that are long when compared with, for example, the 4–10 ps required for a single diffusive step by a solvated ion in aqueous solution (13). The well known outer-sphere surface complex formed by bivalent metal cations (for example,  $Ca^{2+}$ ) in the interlayer region of montmorillonite (compare the left

Table 1. Some clay mineral groups

Group	Layer type	Layer charge, $x$	Structural charge balance*	Structural mass balance*
Kaolinite	1:1	<0.01	$x = 4 - n1^\dagger$	$\sum_{i=1}^6 ni = 8^\ddagger$
Illite	2:1	1.4–2.0	$x = 8 - n1 + n4 + n5 + n6^\ddagger$	$\sum_{i=1}^6 ni = 12^\ddagger$
Vermiculite	2:1	1.2–1.8	$x = 8 - n1 + n4 + n5 + n6^\S$	$\sum_{i=1}^6 ni = 12^\ddagger$
Smectite	2:1	0.5–1.2	$x = 8 - n1 + n4 + n5 + n6^\ddagger$	$\sum_{i=1}^6 ni = 12^\ddagger$

\*Based on an  $O_{10}(OH)_8$  (1:1) or  $O_{20}(OH)_4$  (2:1) unit cell formula.

†See text for definitions of  $ni$  ( $i = 1, \dots, 6$ ).

‡The formulas given are dioctahedral clay minerals with bivalent M in the octahedral sheet. For trioctahedral smectite and vermiculite with monovalent M in the octahedral sheet,  $x = 2(8 - n1) - n2 - n3 + n6$  and  $\sum_{i=1}^6 ni = 14$ .

side of Fig. 2) is immobile on the molecular time scale of  $\approx 100$  ps probed by electron spin resonance spectroscopy and by quasielastic neutron scattering (14, 15). These three types of clay mineral surface species—inner sphere complex, outer-sphere complex, and diffuse-layer—represent different modes of adsorption of aqueous cations that contribute to the formation of an electrical double layer on charged siloxane surfaces (3).

**Interlayer Surface Structure by Neutron Diffraction.** The surface species “cartooned” in Fig. 2 emerged conceptually from the results of *in situ* spectroscopic studies (14, 15). The consensus of these studies is that hydrated smectite and vermiculite interlayers are in many ways similar in structure to a concentrated ionic solution (14). Aqueous solution molecular structure, in turn, has been explored especially well over the same time-period by isotopic-difference neutron diffraction (13, 16). In this methodology, isotopic substitution of one or more diffracting atoms is performed (for example, substitution of hydrogen by deuterium in interlayer water) to create differences in coherent neutron scattering cross section that facilitate locating the atom accurately in relation to its dif-

fracting neighbors (13, 16). Isotopic-difference neutron diffraction methods are reviewed concisely by Skipper *et al.* (17) for hydrated 2:1 clay minerals. Neutron diffraction studies of the interlayers in these systems have already provided valuable insight as to molecular structure in the electrical double layer formed on siloxane surfaces (17–19).

Fig. 3 is a visualization of the arrangement of water molecules around  $Ca^{2+}$  adsorbed in the interlayer region of the two-layer hydrate of trioctahedral vermiculite, based on the results of H/D isotopic-difference neutron diffraction experiments (18). Because the water protons could be identified separately from those in the clay mineral structure and were distinguishable from other interlayer atoms, it was possible to show rather clearly that the  $Ca^{2+}$  are octahedrally coordinated to their nearest-neighbor water molecules, as also occurs in concentrated, as opposed to dilute, aqueous solutions of  $CaCl_2$  (13, 18). Moreover, four of the solvating water molecules form hydrogen bonds with the siloxane surfaces, as expected for clay minerals with isomorphic substitutions only in the tetrahedral sheets (12). Because the two-layer hydrate of vermiculite has about eight water molecules per  $Ca^{2+}$  in the interlayer region

**CATION SURFACE SPECIES ON 2:1 LAYER TYPE CLAY MINERALS AND THEIR RESIDENCE TIMES BY SPECTRAL METHODOLOGIES**

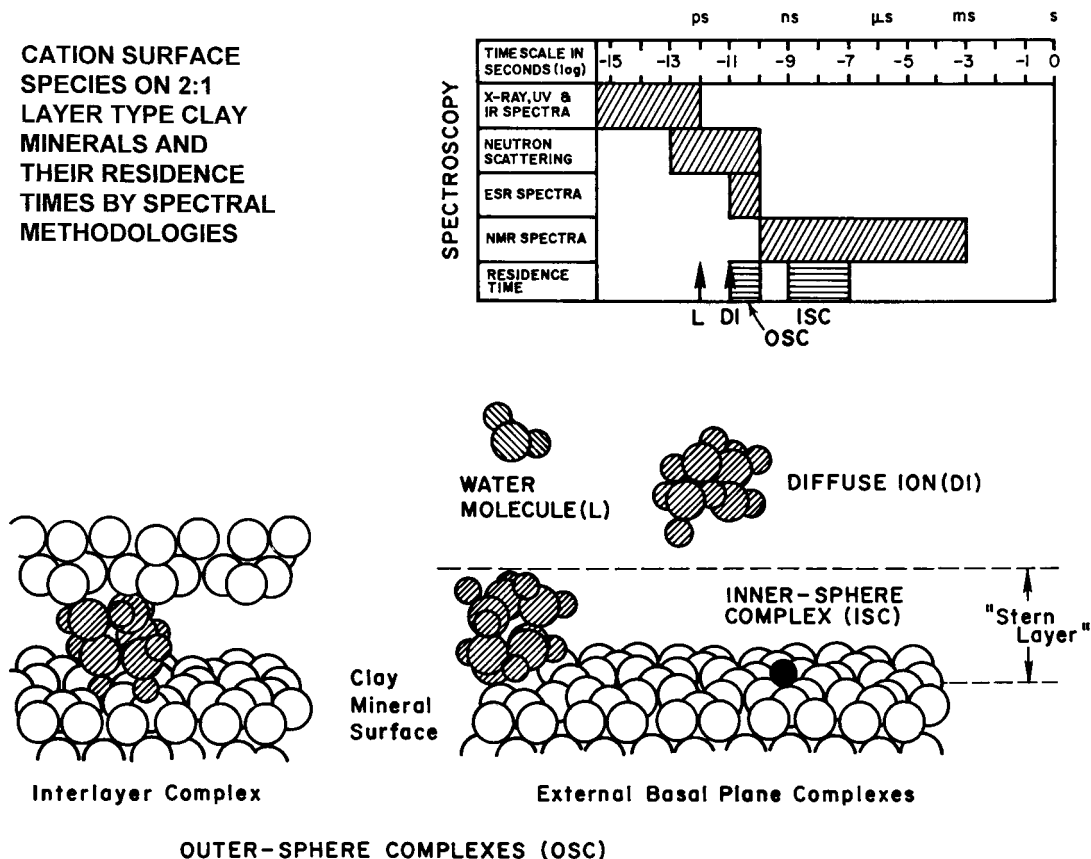


FIG. 2. Cartoon of the three types of small cation adsorption by a 2:1 layer type clay mineral. The “Stern Layer” comprises only surface complexes, which can form in the interlayer region (left) as well as on single siloxane surfaces (right). Characteristic residence time scales of the three adsorbed species are compared at upper right to the time scales of *in situ* spectroscopic methods used to detect them.

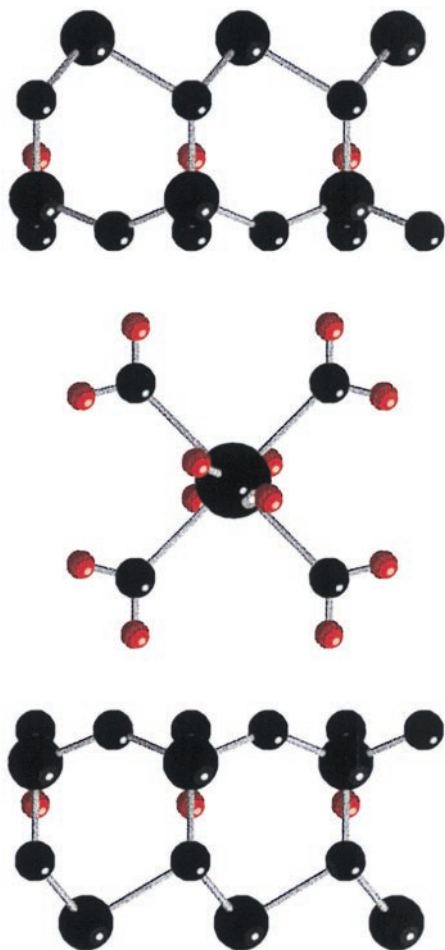


FIG. 3. Visualization of  $\text{Ca}^{2+}$  (large black sphere) in an octahedral solvation complex (water molecules, with smaller black spheres as O and red spheres as H) in the interlayer region of Ca-vermiculite. Portions of the opposing clay mineral layers are shown, with structural protons also indicated in red. Compare to the left side of the cartoon in Fig. 2.

(18), two water molecules per  $\text{Ca}^{2+}$  must be nonsolvating. Skipper *et al.* (18) were able to find these water molecules tucked into the cavities of the siloxane surface. Other neutron diffraction studies of trioctahedral vermiculite hydrates have also reported this phenomenon (17–19).

These structural inferences are in accord with—and improve on—the results of earlier neutron-scattering, electron spin resonance [facilitated by Cu(II) doping], and x-ray diffraction studies of the two-layer hydrate of Ca-vermiculite (20–22), the last of which places  $\text{Ca}^{2+}$  precisely between a triad of surface O on one siloxane surface and a hexagonal cavity in the other. Neutron-scattering and electron spin resonance studies also confirm the immobilization of the interlayer  $\text{Ca}(\text{H}_2\text{O})_6^{2+}$  solvation complex on a 100-ps timescale, which is an order of magnitude longer than a diffusive time step for  $\text{Ca}^{2+}$  in aqueous solution (13).

**Interlayer Surface Structure by Computer Simulation.** Monte Carlo (MC) computer simulations are well known as essential components of research on aqueous ionic solutions (13). The underlying paradigm in these simulations is to construct intermolecular potential functions that represent parametrically all of the known interactions in a system then devise a strategy for sampling the phase space of the interacting system to compute its chemical properties. In a typical MC simulation, the configuration space of the system is sampled randomly under the guidance of an algorithm based in equilibrium statistical mechanics (23). Convergence of the

simulation is monitored by examining the stability of calculated system properties (for example, the layer spacing in the case of hydrated clay minerals) as sampling proceeds.

The synergistic relationship between experiment and molecular modeling indigenous to the study of aqueous ionic solutions has not been possible in the study of hydrated clay minerals until very recently, directly after the appearance of fourth-generation supercomputers and the emergence of convenient parametric models for water–smectite and cation–smectite potential functions based on quantum mechanical insight (24–26). These developments encouraged the undertaking of systematic simulation studies of low-charge smectite hydrates, particularly the ubiquitous Wyoming montmorillonites, which have both octahedral and tetrahedral charge sites (6, 27–34). Prototypical Wyoming montmorillonite corresponds to  $n_1 = 7.75, n_2 = 3.75, n_3 = n_4 = 0, n_5 = 0.5, n_6 = 0$  in the chemical formula given above for 2:1 layer type clay minerals, with  $x = 0.75$  as the layer charge. The results of these simulations have generated a number of fundamental questions that require additional molecular-scale experimentation, thus sustaining the theory–experiment dialogue that defines fundamental geochemical research. The computer simulations summarized in the present article were performed by using the code MONTE (35), developed by N. T. Skipper and K. Refson, with phase-space sampling strategies as described by Skipper *et al.* (27, 28) and Chang *et al.* (25, 26). Figs. 4 and 5 are “snapshots” of equilibrium interlayer configurations based on MC simulations (34) of the two-layer hydrates of Na- and K-Wyoming montmorillonite. The species shown in Fig. 4 is  $\text{Na}^+$  bound in an outer-sphere surface complex to an octahedral charge site of the clay mineral. This visualization, like Fig. 3, confirms the spectroscopy-inspired cartoon in Fig. 2. Fig. 4 includes only water molecules in a solvation shell confined to within 3.2 Å of the central  $\text{Na}^+$ , the individual Na– $\text{H}_2\text{O}$  separations varying from 2.2 to 2.5 Å. These vicinal water molecules form a distorted octahedron, in agreement with Na– $\text{H}_2\text{O}$  distances and coordination numbers determined for concentrated NaCl solutions with the same  $\text{H}_2\text{O}/\text{Na}$  ratio  $\approx 10$  (13). Fig. 5 illustrates  $\text{K}^+$  bound in an inner-sphere surface complex to an octahedral charge site on Wyoming montmorillonite. Portions of both siloxane surfaces are shown, and, in this case, water molecules both within and outside the primary solvation shell of  $\text{K}^+$  (K–O separations varying from 2.8 to 3.7 Å) are depicted. The coordination number of  $\text{K}^+$  with O is eight, but two are contributed by oxygen ions in the siloxane surface. Thus,  $\text{K}^+$  is in distorted cubic coordination with its neighboring O, consistent with geometric concepts based on the  $\text{K}^+/\text{O}$  radius ratio (3).

Strongly solvating monovalent cations like  $\text{Na}^+$  or  $\text{Li}^+$  have a tendency to form only inner-sphere surface complexes with tetrahedral charge sites and only outer-sphere surface complexes with octahedral charge sites on smectites (28, 33). This trend can be related to partial desolvation facilitated by the smaller distance of closest approach between an interlayer cation and a charge site that exists for a tetrahedral as opposed to an octahedral site, which necessarily lies deeper in the clay layer. For large cations like  $\text{K}^+$ , however, the desolvation process is always facile because of a weak interaction with water molecules (13, 31), and inner-sphere surface complexation is not so dependent on the location of the charge site in the clay layer.

Fig. 6 is a snapshot, based on MC simulation (33), of the interlayer configuration in Li-hectorite, a trioctahedral smectite having only octahedral charge sites. The view in the figure is along the clay layer *c* axis, with only one of the two opposing siloxane surfaces shown but with all cations and water molecules in a MC simulation cell depicted. This stable hectorite hydrate, which has been investigated extensively by a variety of spectroscopic techniques, has an average of three water molecules per  $\text{Li}^+$ , which corresponds to a very concentrated ionic

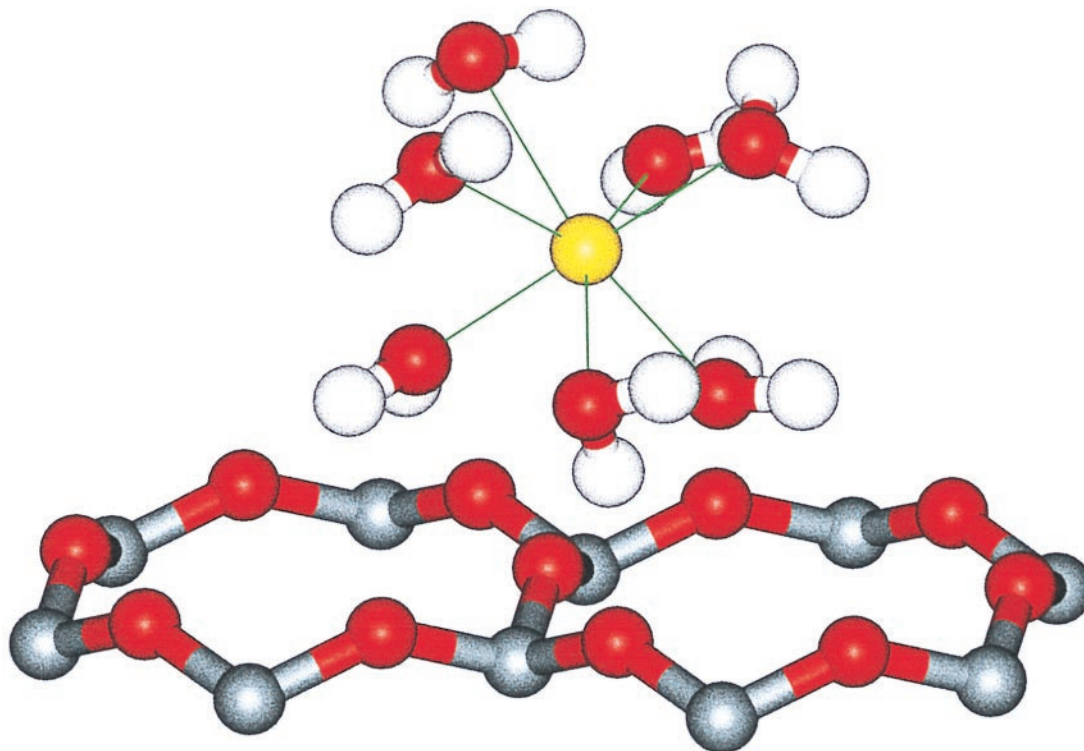


FIG. 4. Visualization of  $\text{Na}^+$  bound in an outer-sphere surface complex in the interlayer region of Wyoming montmorillonite, based on MC simulation. A portion of the siloxane surface structure also is shown.

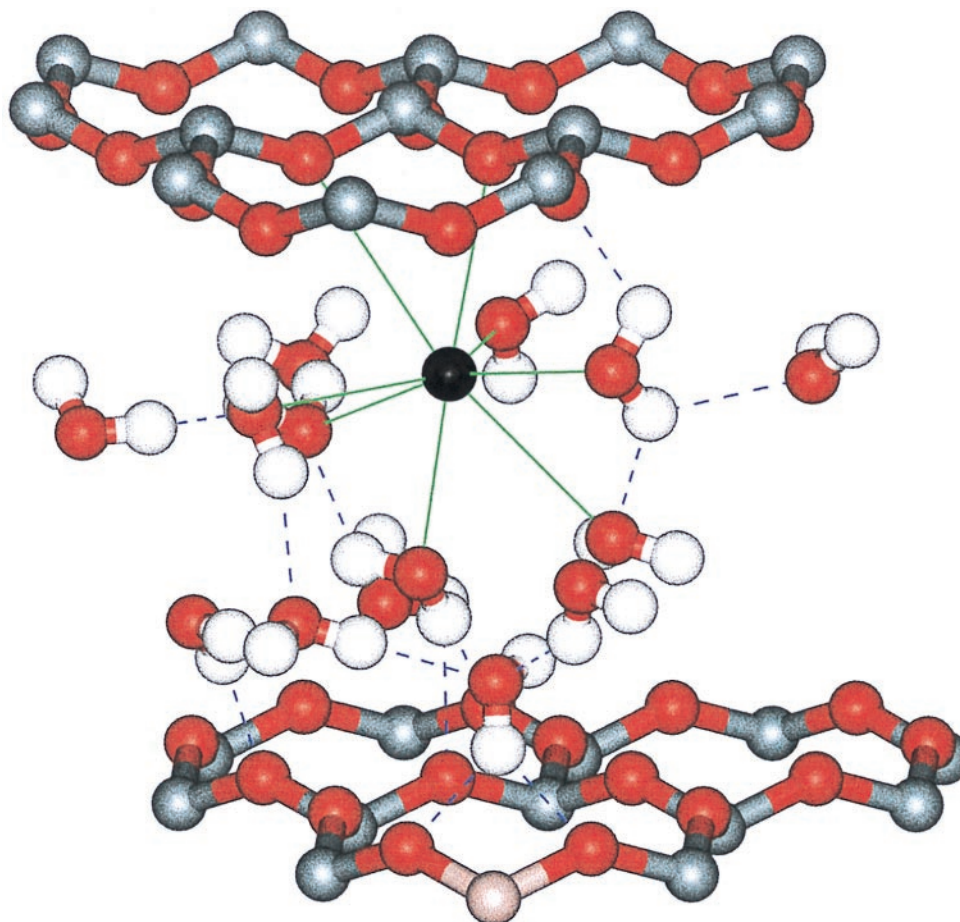


FIG. 5. Visualization of  $\text{K}^+$  bound in an inner-sphere surface complex in the interlayer region of Wyoming montmorillonite, based on MC simulation. Green lines extend from  $\text{K}^+$  (black sphere) to nearest-neighbor O in the surface complex. Dashed lines indicate hydrogen bonds between water molecules. Portions of the opposing two siloxane surfaces also are shown, with the beige sphere at the bottom of the figure (center) indicating a site of  $\text{Al}^{3+}$  substitution for  $\text{Si}^{4+}$ .

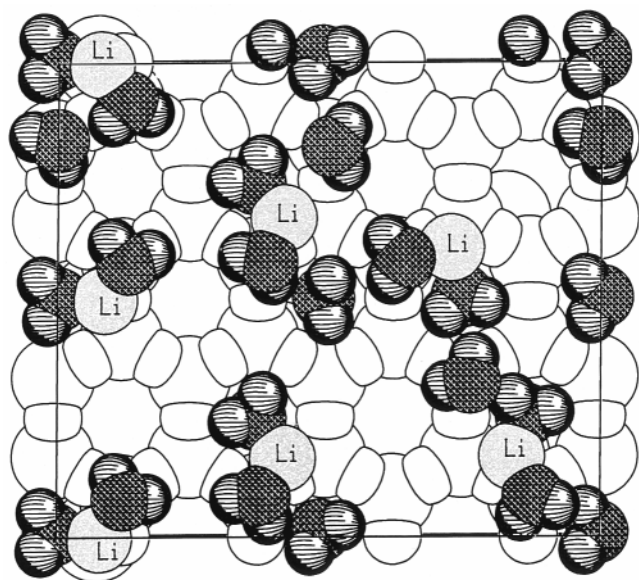


FIG. 6. Visualization of the interlayer configuration in  $\text{Li}(\text{H}_2\text{O})_3$ -hectorite, based on MC simulation (33). The  $\text{Li}^+$  are bound in outer-sphere surface complexes with two water molecules. Other water molecules are keyed into the siloxane surface cavities.

solution ( $\approx 18.5$  molal). Fig. 6 conforms to the trend expected for small interlayer cations, in that only outer-sphere surface

complexes have formed, comprising just two solvating water molecules, in agreement with the average hydration number of 2.3 found in isotopic-difference neutron diffraction studies of very concentrated  $\text{LiCl}$  solutions (16). The nonsolvating water molecules have keyed themselves into the hexagonal cavities of the siloxane surface (one such molecule is at the center of the simulation cell), reminiscent of the situation in trioctahedral vermiculite (17–19).

Much experimental and theoretical information points to an inherent hydrophobicity of the siloxane surface [see, for example, the summary by Jaynes and Boyd (36)] were it not for the presence of layer charge. Pyrophyllite, the uncharged analog of montmorillonite, and talc, the uncharged analog of vermiculite, both have hydrophobic siloxane surfaces (36, 37). Studies of the effect of layer charge on the adsorption of both water and hydrocarbon molecules by smectites (36, 38) indeed show that surface hydrophobicity increases as the layer charge decreases. Recent molecular dynamics simulations of ion solvation and mobility in aqueous solution (39, 40) suggest that large cations like  $\text{K}^+$  tend to interact with water molecules not only through their positive charge but also through solvent cage formation, which is just what hydrocarbon molecules do (41–43). This hydrophobic tendency may be the basis for  $\text{K}^+$  associating directly with clay mineral O (Fig. 5) instead of forming a well organized solvation complex near octahedral charge sites, as does  $\text{Na}^+$  in Fig. 4. Fig. 7 exposes the inherent hydrophobicity of the siloxane surface even more directly through a MC snapshot of a methane molecule adsorbed in the interlayer region of the three-layer hydrate of Na-montmoril-

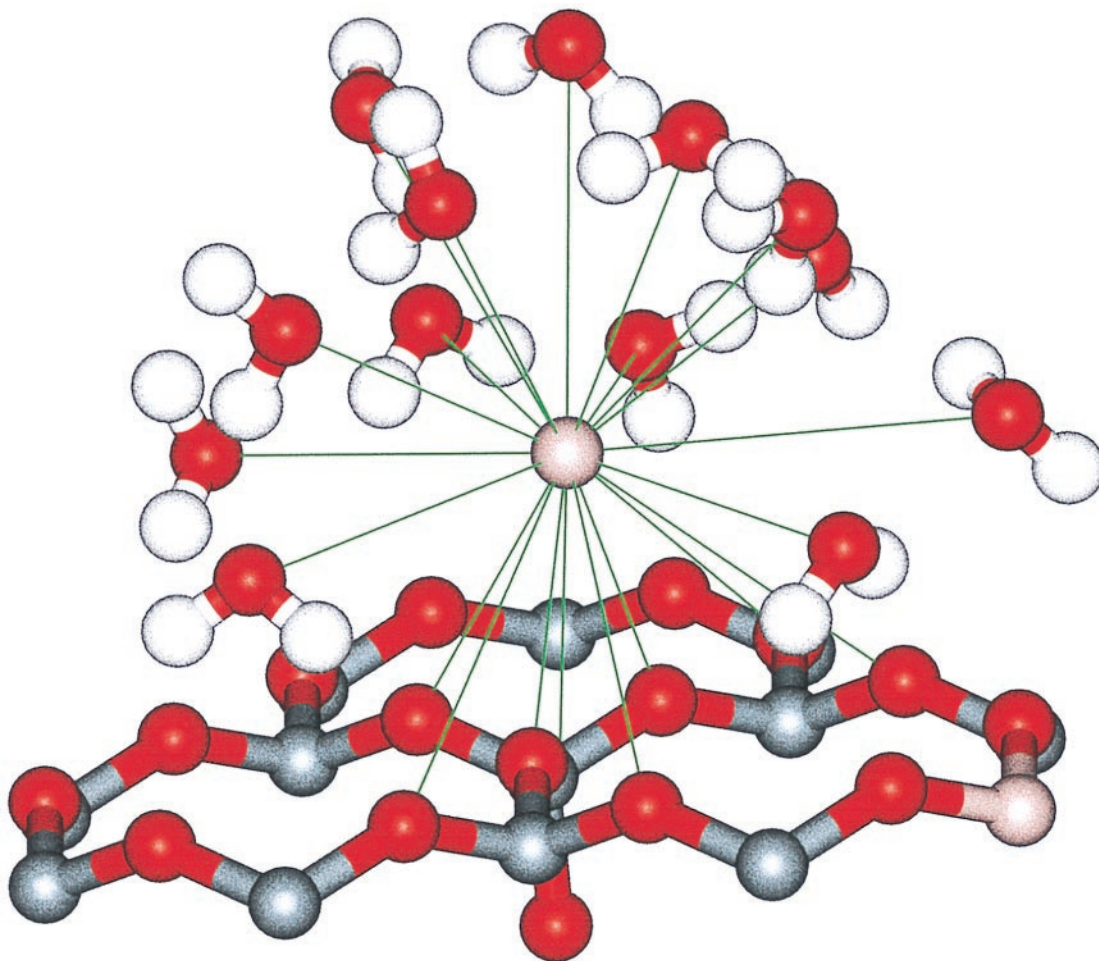


FIG. 7. Visualization of a methane molecule adsorbed in the interlayer region of the three-layer hydrate of Na-montmorillonite, based on MC simulation. The typical 20-fold coordination between  $\text{CH}_4$  and O occurs, but with nearly half of the O being in the siloxane surface.

lonite ( $\text{H}_2\text{O}/\text{CH}_4 = 23$ ). The well known 20-fold coordination cage induced by  $\text{CH}_4$  in bulk water (41, 42) was reproduced successfully by the  $\text{CH}_4$ -O potential function used in the MC simulation (43). In the interlayer of a Na-montmorillonite hydrate, however, methane coordinates to eight clay mineral O and approximately a dozen water molecule O to form this cage in a highly distorted coordination structure. This kind of hydrophobic association, which may be favored for  $\text{CH}_4$  over a purely solvent-based arrangement of neighboring O atoms, could play an important role in the chemical evolution of organic molecules as mediated by clay minerals (44).

The multifaceted nature of interactions within clay mineral interlayers leads necessarily to complexity in the structure of adsorbed water. This complexity is well illustrated by a consideration of water molecule orientations in the two-layer hydrate of Na-montmorillonite as revealed by MC simulation (29). Sodium-water molecule interactions in this system produce a local coordination structure like that in concentrated aqueous solutions of NaCl (13, 29), but  $\text{Na}^+$  interactions with tetrahedral charge sites are still strong enough to allow inner-sphere surface complex formation with oxygen ions in the siloxane surface. The configuration of water molecules differs between inner-sphere and outer-sphere surface complexes. When these two species are forced to cohabit within the constrained spatial domain that exists in an interlayer region, disorder in the water network is likely, with distorted H-bonds and an array of water dipole orientations taking on almost every possible direction (29). This disorder is enhanced by an evident attraction between water molecules and the cavities in the siloxane surface, which gives rise to nonsolvating water molecules keyed into these holes irrespective of the type of adsorbed cation (6, 18, 19, 29–31, 33). The characteristics of adsorbed water on 2:1 clay minerals also reveal the competition between interlayer cations and clay mineral structure for intercalated water molecules, as well as that between hydrophilic and hydrophobic interactions. This competition produces a complex electrical double layer structure whose origins and behavior are beginning to be understood at a fundamental level as the basis for progress toward improved design in applications (7, 8) that provide palpable benefits for humankind.

Without the unflinching support of Dr. John Maccini (U.S. National Science Foundation) and Dr. Sally Benson (Lawrence Berkeley National Laboratory), the simulation research described herein would not have been possible. The authors thank the National Energy Research Scientific Computing Center for allocations of time on its Cray supercomputers and Angela Zabel for excellent preparation of the typescript. The research reported in this paper was supported in part by National Science Foundation Grant EAR-9505629 and in part by the Director, Office of Energy Research, Office of Basic Energy Sciences, Geosciences Division of the U.S. Department of Energy under Contract DE-AC03-76SF00098.

1. Pauling, L. (1930) *Proc. Natl. Acad. Sci. USA* **16**, 123–129, 578–582.
2. Hendricks, S. B. & Fry, W. H. (1930) *Soil Sci.* **29**, 457–479.
3. Sposito, G. (1989) *The Chemistry of Soils* (Oxford Univ. Press, New York).
4. Michalopoulos, P. & Aller, R. C. (1995) *Science* **270**, 614–617.
5. McCauley, S. E. & DePaolo, D. J. (1997) in *Tectonic Uplift and Climate Change*, ed. Ruddiman, W. F. (Plenum, New York), pp. 427–467.
6. Karaborni, S., Smit, B., Heidug, W., Urai, J. & van Oort, E. (1996) *Science* **271**, 1102–1104.
7. Kajita, L. S. (1997) *Clays Clay Miner.* **45**, 609–617.
8. Zielke, R. C., Pinnavaia, T. J. & Mortland, M. M. (1989) in *Reactions and Movement of Organic Chemicals in Soils*, ed. Sawhney, B. L. & Brown, K. (Soil Science Society of America, Madison), pp. 81–97.

9. Bailey, S. W., ed. (1988) *Hydrous Phyllosilicates* (Mineralogical Society of America, Washington, D.C.).
10. Moore, D. M. & Reynolds, R. C. (1997) *X-Ray Diffraction and Identification and Analysis of Clay Minerals* (Oxford Univ. Press, New York).
11. Borchardt, G. (1989) in *Minerals in Soil Environments*, ed. Dixon, J. B. & Weed, S. B. (Soil Science Society of America, Madison, WI), pp. 675–727.
12. Sposito, G. (1984) *The Surface Chemistry of Soils* (Oxford Univ. Press, New York).
13. Ohtaki, H. & Radnai, T. (1993) *Chem. Rev. (Washington, D.C.)* **93**, 1157–1204.
14. Sposito, G. & Prost, R. (1982) *Chem. Rev. (Washington, D.C.)* **82**, 553–573.
15. Sposito, G. (1993) *Ion Exch. Solv. Extr.* **11**, 211–236.
16. Neilson, G. & Enderby, J. E. (1989) *Adv. Inorg. Chem.* **34**, 195–217.
17. Skipper, N. T., Soper, A. K. & McConnell, J. D. C. (1991) *J. Chem. Phys.* **94**, 5751–5760.
18. Skipper, N. T., Soper, A. K. & Smalley, M. V. (1994) *J. Phys. Chem.* **98**, 942–945.
19. Skipper, N. T., Smalley, M. V., Williams, G. D., Soper, A. K. & Thompson, C. H. (1995) *J. Phys. Chem.* **99**, 14201–14204.
20. Tuck, J. J., Hall, P. L., Hayes, M. H. B., Ross, D. K. & Hayter, J. B. (1985) *J. Chem. Soc. Faraday Trans. 1* **81**, 833–846.
21. McBride, M. B. (1986) in *Geochemical Processes at Mineral Surfaces*, ed. Davis, J. A. & Hayes, K. F. (Am. Chem. Soc., Washington, D.C.), pp. 362–388.
22. Slade, P. G., Stone, P. A. & Radoslovich, E. W. (1985) *Clays Clay Miner.* **33**, 51–61.
23. Allen, M. P. & Tildesley, D. J. (1987) *Computer Simulation of Liquids* (Clarendon, Oxford).
24. Skipper, N. T., Refson, K. & McConnell, J. D. C. (1989) *Clay Miner.* **24**, 411–425.
25. Skipper, N. T., Refson, K. & McConnell, J. D. C. (1991) *J. Chem. Phys.* **94**, 7434–7445.
26. Skipper, N. T., Refson, K. & McConnell, J. D. C. (1993) in *Geochemistry of Clay-Pore Fluid Interactions*, eds. Manning, D. C., Hall, P. L. & Hughs, C. R. (Chapman & Hall, London), pp. 40–61.
27. Skipper, N. T., Chang, F.-R. C. & Sposito, G. (1995) *Clays Clay Miner.* **43**, 285–293.
28. Skipper, N. T., Sposito, G. & Chang, F.-R. C. (1995) *Clays Clay Miner.* **43**, 294–303.
29. Chang, F.-R. C., Skipper, N. T. & Sposito, G. (1995) *Langmuir* **11**, 2734–2741.
30. Chang, F.-R. C., Skipper, N. T. & Sposito, G. (1997) *Langmuir* **13**, 2074–2082.
31. Chang, F.-R. C., Skipper, N. T. & Sposito, G. (1998) *Langmuir* **14**, 1201–1207.
32. Boek, E. S., Coveney, P. V. & Skipper, N. T. (1995) *J. Am. Chem. Soc.* **117**, 12608–12617.
33. Greathouse, J. & Sposito, G. (1998) *J. Phys. Chem. B* **102**, 2406–2414.
34. Sposito, G., Park, S.-H. & Sutton, R. (1999) *Clays Clay Miner.*, in press.
35. Skipper, N. T. (1996) *MONTE User's Manual* (Department of Physics and Astronomy, University College, London).
36. Jaynes, W. F. & Boyd, S. A. (1991) *Clays Clay Miner.* **39**, 428–436.
37. Bridgeman, C. H., Buckingham, A. D., Skipper, N. T. & Payne, M. C. (1996) *Mol. Phys.* **89**, 879–888.
38. Sposito, G., Prost, R. & Gaultier, J.-P. (1983) *Clays Clay Miner.* **31**, 9–16.
39. Lynden-Bell, R. M. & Rasaiah, J. C. (1997) *J. Chem. Phys.* **107**, 1981–1991.
40. Koneshan, S., Rasaiah, J. C., Lynden-Bell, R. M. & Lee, S. H. (1998) *J. Phys. Chem. B* **102**, 4193–4204.
41. Swaminathan, S., Harrison, S. W. & Beveridge, D. L. (1978) *J. Am. Chem. Soc.* **100**, 5705–5712.
42. Swaminathan, S., Harrison, S. W. & Beveridge, D. L. (1979) *J. Am. Chem. Soc.* **101**, 5832–5833.
43. Skipper, N. T., Bridgeman, C. H., Buckingham, A. D. & Mancera, R. L. (1996) *Faraday Discuss. Chem. Soc.* **103**, 141–150.
44. Cairns-Smith, A. G. (1982) *Genetic Takeover and the Mineral Origins of Life* (Cambridge Univ. Press, New York).